



Research question: *Evaluating Imaging-Based Techniques for Diagnosis and Analysis of Lung Adenocarcinoma*

Author: Siyona Haldar

Index

Sr. No	Particulars	Page No.
1	Abstract	1
2	Keywords	2
3	Introduction	2
4	Literature Review	4
5	Methodology	9
6	Findings and Discussion	14
7	Conclusion	19
8	References	23

Abstract

This study explores current imaging-based techniques involved in the diagnosis of Lung Adenocarcinoma (LUAD), one of the most common forms of lung cancer. Diagnosis of LUAD includes the use of techniques, such as MRI, CT, PET-CT and CECT to identify and treat malignant tumours. This research compares the ability of each diagnosis technique to track positive cases of LUAD. It analyses between CECT, CT and PET-CT in terms of recognising the number of TP, TN, FP and FN cases reported. The paper shows that in terms of LUAD and LUSC, Gene expression analysis revealed higher ENO1 levels in LUSC, indicating greater FDG uptake and suggesting that PET/CT may be more effective for LUSC than LUAD. These data analyses of other peer-reviewed studies highlight the importance of selecting the right medical tools in clinical contexts. It highlights the importance of diagnostic efficacy within clinical contexts and the need for new ways to improve detection accuracy. Overall, the study shows a multi-leveled relationship between tumour biology and diagnostic performance, which can be harnessed to aid the diagnosis of Lung Adenocarcinoma.

Keywords:

Lung Adenocarcinoma; Epidermal Growth Factor Receptor (EGFR); Kristen Rat Sarcoma Viral Oncogene Homolog (KRAS); Non-Small Cell Lung Cancer (NSCLC); Mucosal Glands; Chronic Inflammation; Cellular Damage; Body's Immune Response; Low Growth Rate; Cancer Diagnosis; Symptoms of Lung Adenocarcinoma; Medical Imaging; Computed Tomography (CT); Positron Emission Tomography (PET); Magnetic Resonance Imaging (MRI); Tumour Progression; Survival Rate; Risk Factors; Lung Cancer Symptoms; Molecular Testing; EGFR Mutations; Diagnostic Techniques; FDG-PET; Fludeoxyglucose; Phosphorylation; Radioisotope; Inflammatory; PET-CT; Metastasis; Superior Sulcus Tumours; Chest Wall Invasion; Brachial Plexus Involvement; Pancoast Tumour; Lung Parenchyma; True Positive; True Negative; False Positive; False Negative; Patient Heterogeneity; Statistical Validation; Diagnostic Odds Ratio (DOR); ENO1; Glycolytic Enzyme; Glucose Metabolism; Gene Expression; Metabolism Markers; Early-Stage Disease; Non-Small Cell Lung Cancer (NSCLC); Single-Cell RNA-Sequencing; Lung Squamous Cell Carcinoma (LUSC)

Introduction:

Identifying What Lung Adenocarcinoma (LUAD) Refers to

Lung Adenocarcinoma is one of the most common and life-threatening types of lung cancer that can occur in people. It accounts for 40% of all lung cancers. LUAD is classified as a non-small cell lung cancer (NSCLC) and occurs in the lung margin. Epithelial cells responsible for the generation of mucus are typically associated with cancerous transformation and the development of LUAD (Jacks et al., n.d.).

LUAD begins when normal lung cells start to change and grow abnormally (Rosell et al., 2023). This often happens due to mutations in specific genes. One of the most common is Epidermal Growth Factor Receptor (EGFR), which causes cells to grow too quickly. Another is the Kristen Rat Sarcoma Viral Oncogene Homolog (KRAS), which prevents cells from stopping division even when they should (Rosell et al., 2023). The loss of TP53, a gene that usually prevents damaged cells from multiplying, also plays a major role (Carel Medical Benefits Management, 2022). Environmental exposures, such as tobacco smoke and air pollution, increase the chances of changes in the genes occurring (Pahwa et al., 2023).

Furthermore, LUAD can occur from areas of chronic inflammation in the lungs (Lung Cancer Foundation of America, n.d.). Inflammation plays an important role in the body's defense system. It removes any dangerous foreign substances. Additionally, inflammation is responsible for the healing process (Pahwa et al., 2023). In terms of lung cancer, persistent or chronic inflammation can contribute to cellular damage, genetic mutations and tumour progression (Nishida & Andoh, 2025). LUAD has a low growth rate and is more susceptible to

detection before spreading significantly to various parts of the body (Lung Cancer Foundation of America, n.d.).

Understanding How Common Lung Adenocarcinoma is Amongst Men and Women

LUAD is highly dangerous for both men and women in various parts of the world, as this type of cancer poses a significant challenge to minimise the cancer's risks. (World Cancer Research Fund, n.d.). Research shows that Lung Adenocarcinoma was the highest number of cases diagnosed in the United States of America in 2021. Despite the decline in the number of cases and deaths compared to the previous years, LUAD is still responsible for the majority of cancer deaths in the United States of America. Lung cancer was equivalent to 45% of all lung cancer cases in the United States of America in the year 2021 (CDC, 2025).

Similarly, in Spain, LUAD is regarded as the most common tumour for both men and women (Remon et al., 2021). Research pinpoints that it is more prevalent in women, and non-smoking women are twice as likely to be diagnosed with LUAD than men. Therefore, it is crucial to know that while smoking is a major risk factor for LUAD, this type of lung cancer is also found in non-smokers (Barrera-Rodriguez & Morales-Fuentes, 2012). In these non/never-smokers, other possible causes include air pollution. Since air pollution comprises a combination of harmful particles, there are several ways it could lead to lung cancer. For instance, small particles can accumulate in the lungs and harm the DNA within cells. This may alter the way cells replicate, potentially resulting in cancer (The Francis Crick Institute, 2022).

Explaining Why LUAD is An Issue

LUAD poses a significant threat worldwide due to a rise in the number of cases. Studies have highlighted that it is the principal cause of cancer death in men and the second cause of cancer death in women. For example, data shows that in 2018, there were 1.8 million deaths worldwide due to Lung Adenocarcinoma - 1.2 million deaths were men and 576,100 deaths were women (Schabath & Cote, 2019).

LUAD has a high mortality rate, making it one of the deadliest forms of lung cancer. Its prevalence is also increasing globally, raising serious public health concerns. The majority of patients eventually die from the disease (Yang et al., 2022). Despite medical advancements, lung adenocarcinoma survival remains limited. According to SEER analysis for the years 2015 to 2021, the overall 5-year relative survival rate for non-small cell lung cancer (the category that includes adenocarcinoma) is 32%, with localised cases. This means the cancer being detected and diagnosed at an early stage has a 67% 5-year survival and 12% for distant disease, where the cancer has spread to remote organs such as the brain, liver, or bones. However, only about 23% of

lung cancers are diagnosed at a localised stage. This indicates a significant barrier to early intervention (American Lung Association, n.d.).

Recognising the Symptoms Associated With LUAD

Lung cancer can cause various symptoms, and these can vary depending on the stage of the disease (Myers & Wallen, 2023). According to research, some of the most common symptoms include a long-lasting cough, coughing up blood (known as hemoptysis), chest pain and swelling in the face. People can experience trouble with their breathing (called dyspnea), have swollen lymph nodes near the neck or collarbone, and undergo weight loss). They can feel tired, feel pain from the cancer that has spread, and at times have a fever. In some cases, cancer can cause other symptoms, such as Horner syndrome (Xing et al., 2019). Horner syndrome is a neurological condition which is characterised by three main symptoms. They are known as ptosis (this means drooping eyelid), miosis (which is constricted pupil), and anhidrosis (loss of sweating). The symptoms are a result of disruption of the sympathetic nerve pathway, which is associated with tumours at the lung apex, such as in LUAD (Khan & Bollu, 2023).

The symptoms depend on how advanced the cancer is. In early stages, there might be no signs at all. Doctors may only find a lung nodule during a scan done for another medical reason. In later stages, more noticeable symptoms such as a cough that remains persistent, coughing up blood and experiencing significant weight loss are more common (Myers & Wallen, 2023).

Literature Review:

Analysing the Diagnostic Procedures of LUAD

The diagnosis of lung cancer usually begins with imaging, due to tissue inaccessibility (Nooreldeen & Bach, 2021). Low-Dose CT (LDCT) scans are effective in detecting cancer early and lowering mortality in high-risk groups (National Lung Screening Trial Research Team, 2011). High-Resolution CT (HRCT) is the preferred method for evaluating suspicious lung lesions (Carelon Medical Benefits Management, 2022). On another level, PET-CT helps assess cancer spread and activity. In advanced cases, brain MRI is often performed due to the risk of metastases, particularly in lung adenocarcinoma (Feng et al., 2024).

A confirmed diagnosis requires tissue sampling. This can be through CT-guided needle biopsy, bronchoscopy, or endobronchial ultrasound (EBUS) (Ettinger et al., 2022; Travis et al., 2015). Once LUAD is identified, molecular testing is done to check for mutations, such as Epidermal Growth Factor Receptor (EGFR), Anaplastic Lymphoma Kinase (ALK), Kirsten Rat Sarcoma Viral Oncogene Homolog (KRAS) and

ROS Proto-Oncogene 1 (ROS1) (Lindeman et al., 2013; Skoulidis & Heymach, 2019). EGFR, ALK, KRAS and ROS1 are genes that encode proteins which are involved in cell growth, signaling pathways, mutations or rearrangements. These genes are commonly associated with lung adenocarcinoma (Herbst et al., 2018).

Therefore, identifying specific mutations helps guide targeted treatments for patients (Mok et al., 2017). However, some mutations, such as those in the KRAS gene, are linked to resistance against certain therapies, making LUAD more difficult to treat (Nooreldeen & Bach, 2021). KRAS mutations in LUAD can confer resistance to therapies by altering the structure of the KRAS protein. This causes it to remain in an active state and drive cancer cell proliferation even in the presence of targeted drugs. These mutations also lead to resistance against EGFR-targeted therapies, such as gefitinib and erlotinib. Furthermore, KRAS mutations can influence the effectiveness of other therapies, including immunotherapy (Xie et al., 2021).

People who are over 60 years old comprise the majority of cases (Howlader et al., 2023). The diagnostic approach remains similar, but it may be adjusted based on an individual's overall health (Corre et al., 2016). For instance, less invasive methods, such as liquid biopsy, are sometimes preferred for frail individuals (Aggarwal et al., 2019). Additionally, a comprehensive geriatric assessment may also be used to balance the risks and benefits of testing in older adults (Corre et al., 2016).

Investigation Imaging-Based Techniques for Diagnosis and Analysis

Medical Imaging is the process of visual presentation of various organs and tissues in the human body to monitor and detect abnormal anatomy and physiology of the body. There are several imaging-based techniques which can be used for this purpose. This includes Chest X-ray, Computed Tomography (CT), Positron Emission Tomography (PET) and Magnetic Resonance Imaging (MRI) (Hussain et al., 2022).

The Advantages of Using Chest X-ray for Diagnosing and Analysing Lung Adenocarcinoma

Chest X-ray is the first-line imaging tool which is used when LUAD is suspected. This is due to its widespread availability, low cost and ability to reveal abnormalities in the lung fields (NHS, 2025). Chest X-ray works by using a controlled dose of ionising radiation to produce images of the chest, where denser structures such as tumours appear white against the darker background of air-filled lungs (RadiologyInfo Org, 2024). In cases of LUAD, chest X-rays may reveal peripheral lung opacities, irregular nodules or signs of pleural effusion (RadiologyInfo Org, 2024). These are common features that are associated with this subtype (Aklin et al., 2022).

The Disadvantages of a Chest X-ray

Chest X-rays alone cannot confirm LUAD. They are mainly used as an initial test to spot possible problems. More detailed imaging, such as CT or PET-CT, is needed to confirm the diagnosis. X-rays use radiation to make two-dimensional images of the chest. Tumours appear white, while healthy lungs appear black. Small tumours can be hidden by bones, or other tissues including muscle, fat, tendons and ligaments. As a result, cancer is often found only when it is large and has reached an advanced stage. At that stage, it is harder to treat it. Noncancerous conditions, such as scars or infections, can look similar to cancer on X-rays. Radiologists can see that something is abnormal. However, they cannot confirm cancer without conducting more tests for the patients (Verywell Health, 2023).

The Benefits of Using Computed Tomography

Computed Tomography scanning is a highly reliable option in imaging. This is because of the detailed information which is provided on the tumour's localisation and scope. Additionally, CT scans can help to detect the presence of swollen lymph nodes and other metastatic diseases. It is a critical tool for evaluating nodal involvement (De Wever et al., 2011). Nodal involvement refers to the presence of cancer cells in the lymph nodes. It indicates that the cancer has spread beyond the original site (American Cancer Society, 2025).

Lymph nodes are small bean-shaped glands that filter lymph fluid to trap bacteria, viruses and other foreign substances, including cancer cells (National Cancer Institute, n.d.). These glands are a fundamental aspect of the body's immune system (American Cancer Society, 2025). Therefore, they offer a comprehensive map of lymph node structures in the hilum and the mediastinum. Hilum refers to the central area on each lung where blood vessels, lymph nodes, bronchi and nerves enter and exit. The mediastinum is the central part of the chest cavity between both the lungs. This anatomical guidance is valuable for surgical planning and targeting lymph nodes for biopsy (De Wever et al., 2011).

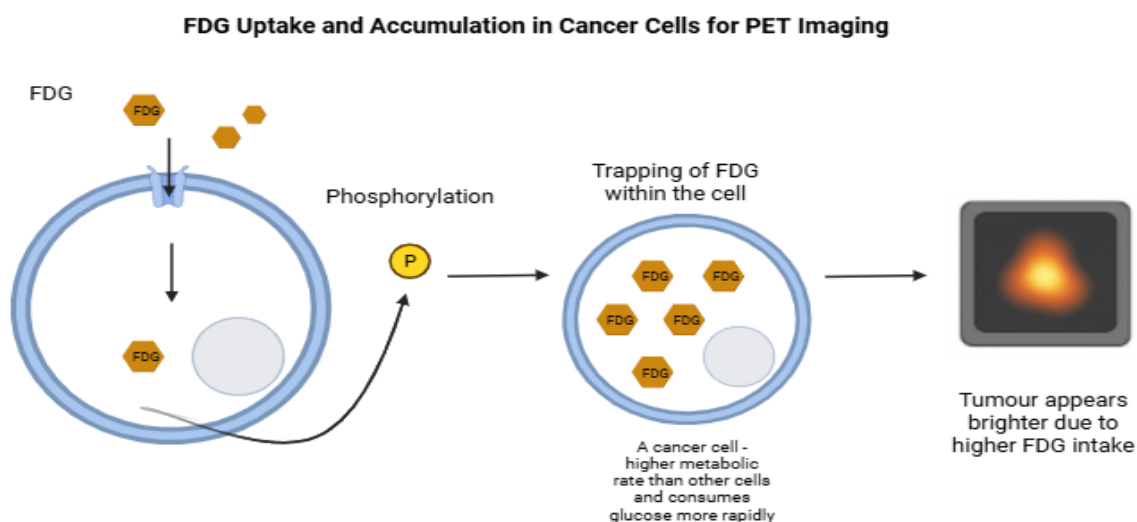
The Negative Aspects of Computed Tomography

While CT scans provide high-resolution images and detailed anatomical information, they have significantly higher radiation exposure. It is up to 50 to 1,000 times more than conventional X-rays. This cumulative radiation dose is especially a concern for patients who require repeated scans for surveillance or staging (Patel & Jesus, 2023). Another disadvantage is the frequent detection of indeterminate pulmonary nodules, which can result in false alarms and lead to unnecessary biopsies or surgical interventions (Gould et al., 2013).

Additionally, Computed Tomography lacks functional or metabolic information. Functional imaging involves changes in the body's active biological processes. The measurements include blood flow, regional chemical composition, and absorption (Fuss & Cheng, 2016). Therefore, making it difficult to distinguish between active tumours and benign lesions (Gould et al., 2013). Research indicates that contrast-enhanced CT scans can pose risks to patients with renal impairment or iodine allergies. Finally, Computed Tomography may still have difficulty detecting microscopic metastases or early brain involvement. This urges the necessity for having supplementary imaging, including PET, CECT and X-ray (Hellwig et al., 2009).

Explaining the Positive Implications of Utilising Positron Emission Tomography

Positron Emission Tomography is a sensitive and specific imaging technique. It functions by using radioisotopes of natural elements, where the most commonly used radioisotope is Fludeoxyglucose (FDG). Similar to regular glucose, FDG is taken up by cells and used as a source of energy. However, once fluoro-deoxy-glucose enters the cell, it goes through a process called phosphorylation. This is where a small chemical group called a phosphate is added to it. This change causes the FDG to get 'stuck' inside the cell because it can no longer be broken down or used further. Since cancer cells use more energy than normal cells, they absorb more Fluorodeoxyglucose (FDG) and light up on the PET scan. It makes it easier to spot the tumours (Boellaard et al., 2015).



Created in BioRender.com bio

Figure X) FDG uptake and trapping in Cancer cells, leading to increased signal intensity on PET scan.

Exploring the Negative Consequences of Utilising Positron Emission Tomography

One of the key limitations in PET-CT is its inability to distinguish between malignancy and inflammatory or infectious conditions, which can result in false positives. These results can display that someone has cancer when they actually do not have it. This may lead to misdiagnosis, additional testing, or people receiving unnecessary treatments. Furthermore, PET-CT is expensive and not readily available, especially in resource-limited settings. It involves radioactive tracers, which may require specialised handling and infrastructure. Additionally, small tumours under 8 – 10 mm may not be detected reliably due to resolution limits. Thus, reducing sensitivity in early-stage disease (Boellaard et al., 2015).

Identifying The Significance of Magnetic Resonance Imaging (MRI)

Magnetic Resonance Imaging (MRI) is especially valuable in assessing central nervous system involvement. This is common in advanced lung adenocarcinoma (Rogers et al., 2021). MRI offers superior soft tissue compared to CT. As a result, it is the imaging method of choice for detecting brain metastases often before the symptoms arise. In addition, MRI is highly effective in evaluating superior sulcus tumours, chest wall invasion and brachial plexus involvement (Yang et al., 2022).

A superior sulcus tumour is also known as a Pancoast tumour. It is a type of lung cancer tumour that stems from the apex (upper part) of the lung. Superior sulcus tumour has the potential to invade nearby structures. This includes the chest wall, ribs, vertebrae and nerves (Gundepalli & Tadi, 2023). On another level, a chest wall invasion refers to tumour involvement in the bones and muscles of the chest wall. This invasion marks a poor prognosis and an advancement in the spread of cancer (UCLA Health, n.d.). Brachial plexus involvement means the injuries to the brachial plexus (Mayo Clinic, 2025). This is a network of nerves originating in the neck and extending into the shoulder, arm and hand (Mayo Clinic, 2025). These injuries can cause a range of symptoms, such as pain, weakness, numbness, or loss of movement in the affected arm and hand (Mayo Clinic, 2025).

These are critical considerations in surgical planning (Melloni et al., 2019). Although MRI is not routinely used for primary lung evaluation, MRI complements CT and PET-CT. This is because it provides detailed imaging of neurologic and soft-tissue metastases (Zhang et al., 2022).

Discovering the Negative Aspects of Using Magnetic Resonance Imaging

MRI can present several challenges in lung cancer imaging. First, it has limited utility for evaluating lung parenchyma due to the presence of air, which causes signal loss and reduced image quality. Second, MRI

scans typically require longer acquisition times, making them uncomfortable for patients, especially those who are claustrophobic or unable to lie still. Motion artefacts caused by breathing can further reduce image clarity. Additionally, MRI is not suitable for patients with certain implants. This includes pacemakers, or people with renal insufficiency, when contrast agents such as gadolinium are needed. Cost and limited availability in smaller healthcare centres can also hinder access to MRI (AJR, 2012). While it is excellent for detecting brain metastases, it is not used routinely for primary lung lesion assessment or detailed evaluation of mediastinal lymph nodes (Yang et al., 2022).

Methodology:

Figure 1: Comparison of Results across FP, FN and TN, in CECT, CT, and PET/CT

1.1 Information about the Secondary Data Source That is Used

This study utilises secondary data, which is derived from a comprehensive systematic review and meta-analysis of diagnostic methods for pulmonary nodules and lung cancer. This is reported in the peer-reviewed literature named as Comparing the diagnostic value of 18F-FDG-PET/CT versus CT for differentiating benign and malignant solitary pulmonary nodules: a meta-analysis. The study was conducted by Jia et al., 2019. Baseline data were extracted from Table 1 of the article titled “*Diagnostic performance of CECT, CT, and PET/CT in evaluating lung nodules*” published in the Journal of Thoracic Disease. The table includes diagnostic performance metrics, such as true positives, true negatives, false positives and false negatives. This is from multiple clinical studies in various countries, such as the United States of America, Korea, China, Japan, Italy, Brazil, Netherlands, Turkey, Israel, Belgium, the United Kingdom, Spain and Poland.

1.2 Data Model and Analytical Approach

The model used in this research paper involves descriptive statistical analysis of diagnostic performance outcomes across three imaging modalities: Contrast-Enhanced CT (CECT), CT and PET/CT. A clustered bar chart was developed to visually compare the average number of true positive, true negative, false positive and false negative cases per study for each diagnostic tool. This visualisation aimed to uncover patterns in diagnostic accuracy and error rates that would be less visible in raw tabular data.

1.3 Details about Sampling Technique and Sample Size

A non-probability purposive sampling method was applied targeting studies that:

- Explicitly reported all four diagnostic outcomes (TP, TN, FP and FN).
- Utilised one of the three imaging tools which are under study.
- Had identifiable sample sizes and gold standard confirmation (for example, histology and biopsy).

The final sample included:

- 13 studies using CECT
- 3 studies using CT
- 23 studies using PET/CT

This resulted in a total of 39 studies that were analysed.

1.4 Data Collection and Processing

Data was manually extracted from the published table and cross-verified for completeness. To address discrepancies in study count and participant numbers between modalities, normalisation was conducted by calculating the average count per study for each diagnostic metric. This adjustment ensures fair comparison across modalities with unequal study representation.

1.5 Formula Inclusion and Exclusion Criteria

Included in the analysis:

- Studies with clear reporting of true/false positives and negatives.
- Studies that used histopathological or cytological confirmation.

Excluded from the analysis:

- Studies with missing or NA values for any diagnostic outcome.
- Studies using hybrid or non-comparable diagnostic tools

This was done to ensure statistical integrity and comparability of outcomes.

1.6 Data Interpretation and Implications

By using average values per study, the chart minimises bias from unequal sample sizes and enables a clearer understanding of which modality tends to perform more reliably on a per-study basis. However, this also means that within-study variability and patient-level heterogeneity are not captured. Patient heterogeneity refers to the natural differences among individuals, which may be explained by factors such as age, employment status, symptoms and treatment preferences. This should be acknowledged as a limitation.

1.7 Statistical Testing and Validation of Data

To evaluate whether there were statistically significant differences in diagnostic performance among the three imaging techniques (CECT, CT and PET/CT), a One-Way ANOVA test was conducted on Excel for each performance metric: true positive, true negative, false positive and false negative rates.

ANOVA (Analysis of Variance) is a statistical method that is used to compare the means of three or more groups to determine if at least one group is significantly different. The F-value represents the ratio of variance

between groups to variance within groups. A higher F-value suggests a greater likelihood of meaningful differences among group means. The p-value indicates the probability that the observed differences occurred by chance. A p-value less than 0.05 is generally considered statistically significant.

In addition to statistical testing, comparative visual analyses were conducted by using bar charts. These visual tools were used to support the interpretation of ANOVA results and highlight any performance trends that may not be statistically significant. However, they are clinically meaningful.

Figure 1.1 illustrates the Diagnostic Odds Ratio (DOR) for each imaging modality - CECT, CT and PET/CT. DOR is a single measure of diagnostic effectiveness and was calculated using the formula:

$$\text{DOR} = (\text{True Positive} / \text{False Negative}) \div (\text{False Positive} / \text{True Negative}).$$
 This metric combines both sensitivity and specificity and provides a comprehensive view of each method's overall diagnostic power.

Figure 1.2 presents the ratio of True Positives to False Negatives for each modality. This was calculated by dividing the number of true positive detections by the number of false negatives:

$$\text{TP/FN Ratio} = \text{True Positive} \div \text{False Negative}.$$
 This ratio helps compare the sensitivity of each diagnostic tool by evaluating how well it detects actual cases without missing them.

Figure 2: ENO1 Gene Expression in LUAD vs. LUSC Patients (Using sSCOPE)

2.1 Information about the Secondary Data Source That is Used

This research uses secondary single-cell transcriptomic data from the peer-reviewed study titled “Phenotype moulding of stromal cells in the lung tumour microenvironment” by Lambrechts et al. (2018), published in Nature Medicine. The data was accessed through the online SCope platform, under the ‘Data Availability’ section of the article. The dataset contains single-cell RNA-sequencing profiles from patients diagnosed with non-small cell lung cancer (NSCLC). This allows cell-level comparison of gene expression across tumour subtypes.

2.2 Data Model and Analytical Approach

This part of the study focuses on comparing the expression of the ENO1 gene, a glycolytic enzyme associated with glucose metabolism, between two lung cancer subtypes: Lung Adenocarcinoma (LUAD) and Lung Squamous Cell Carcinoma (LUSC). The gene expression data was visualised using:

- UMAP projections showing ENO1 expression at the single-cell level using a red-to-black colour scale.

- Boxplots showing per-patient expression levels.

These visualisations help interpret the intensity and variability of ENO1 expression across individual patients grouped by subtype.

2.3 Details about Sampling Technique and Sample Size

A non-probability purposive sampling approach was used to include only tumour-derived cells from four specific patients in the sCOPE dataset:

- LUAD patients: Patient 3 and Patient 4 on study (marked as A and B on Fig. 2 for better comprehensibility)
- LUSC patients: Patient 1 and Patient 2 (marked as A and B on Fig. 2 for better comprehensibility)

Only tumour cells were included to avoid confounding expression signals from non-cancerous tissue or stromal cells. Each patient sample contains hundreds to thousands of individual cells.

2.4 Data Collection and Processing

The sCOPE platform was used to filter and visualise data through the following settings:

- Cell selection: Tumour cells only
- Log transform: ON
- CPM normalisation: OFF
- Expression-based plotting: ON
- Show labels: ON
- Dissociate viewers: ON (to enable side-by-side patient comparison)

Expression sliders were adjusted to visualise the entire range of ENO1 expression. Red colour denoted high expression, and black denoted low/no expression.

2.5 Formula Inclusion and Exclusion Criteria

Included:

- Tumour-derived cells from selected LUAD and LUSC patients.
- Only cells with measurable ENO1 expression levels.

Excluded:

- Non-tumour cells (immune/stromal).
- Patients not relevant to LUAD or LUSC subtypes.

This selection ensured that the analysis directly reflects ENO1 activity in malignant epithelial cells responsible for tumour metabolism.

2.6 Data Interpretations and Implications

Boxplots revealed that LUSC patients (A and B) had higher ENO1 expression compared to LUAD patients (A and B). Since ENO1 is a key glycolysis enzyme, this suggests that glucose metabolism is more active in LUSC tumours. This has implications for the use of FDG-PET imaging, which detects glucose uptake: it may be more effective in LUSC due to higher metabolic activity. This gene-level evidence supports the clinical understanding of how glucose-avid different NSCLC subtypes are.

2.7 Statistical Testing and Validation of Data

No formal statistical test (for example: ANOVA or t-test) was applied in this segment, due to the limited sample size (4 patients). However, visual comparison via boxplots provides clear evidence of ENO1 gene expression trends.

Findings and Discussion:

1. Figures and Results from Figure 1: Comparison of Results across FP, FN and TN in CECT, CT, PET/CT

1.1 Main Findings

The results were tabulated and visualised in a clustered bar chart (see Figure 1). PET/CT had the highest average true positives per study (48.7). However, it was also associated with higher false positives and false negatives. In contrast, CT showed the lowest false positive rate but also the lowest true positive yield, indicating limited sensitivity. CECT offered a balanced performance, with moderate averages across all four diagnostic metrics.

Diagnostic Tool	True Positive	True Negative	False Positive	False Negative
CECT	53.3	32.3	15.8	4.8
CT	28.7	32.0	7.0	6.0

PET/CT	48.7	29.1	10.6	9.0
--------	------	------	------	-----

Table 1

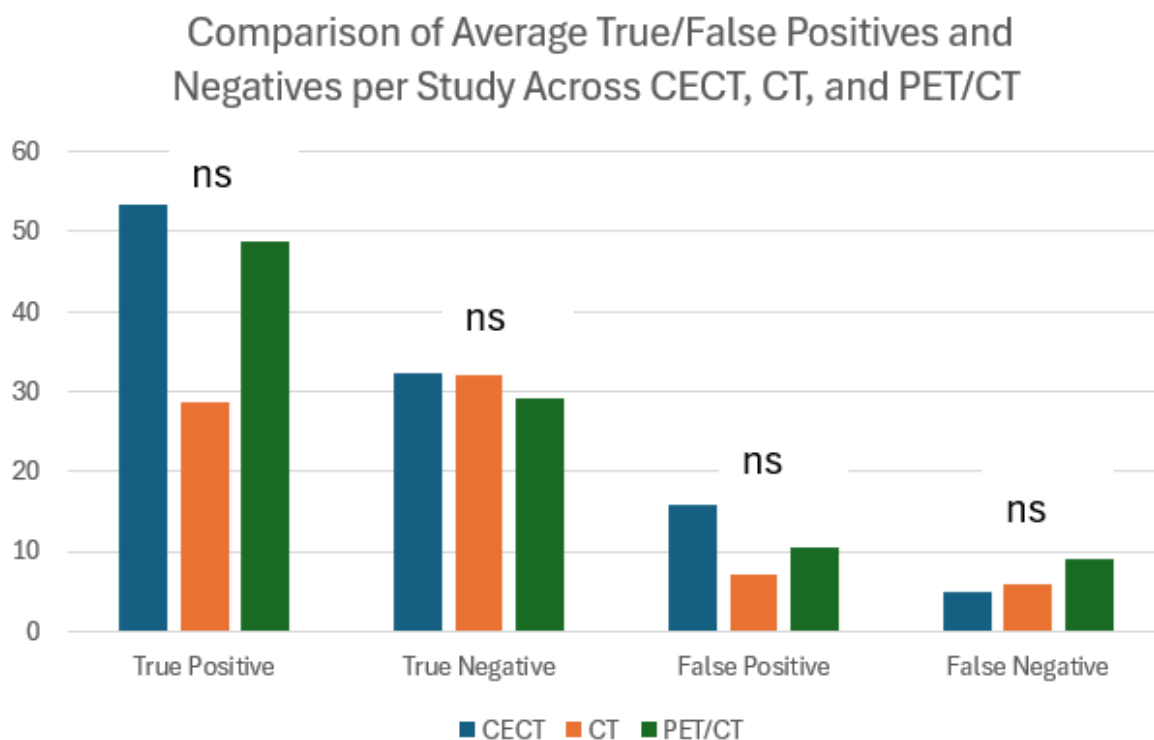


Figure 1) Comparison of average diagnostic outcomes across imaging modalities (CECT, CT, and PET/CT). Bar graph representing the mean number of True Positives (TP), True Negatives (TN), False Positives (FP), and False Negatives (FN) per study for each imaging modality. Statistical analysis was conducted using ordinary one-way ANOVA with a significance threshold set at $p < 0.05$. No statistically significant differences were observed between the groups (ns = not significant).

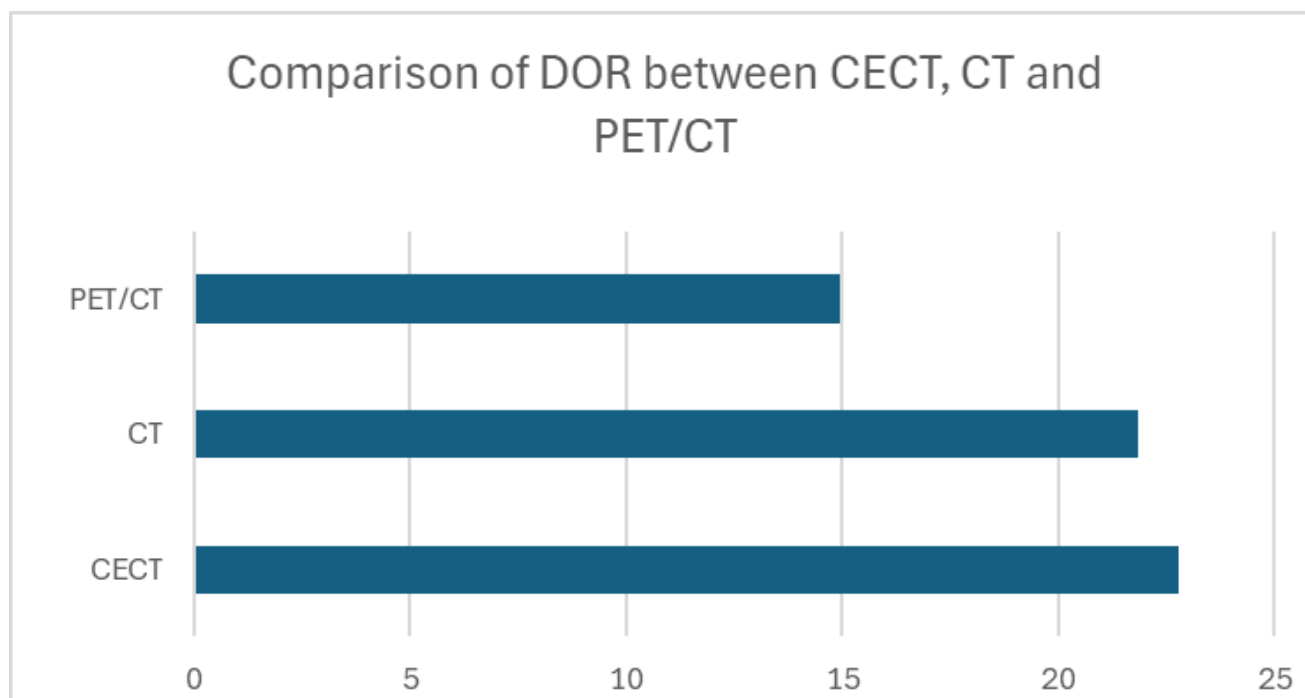


Figure 1a

Figure 1a presents a horizontal bar chart comparing the Diagnostic Odds Ratios (DOR) of CECT, CT, and PET/CT. The results indicate that CECT achieves the highest DOR at approximately 23.9, with CT following closely at about 22.1. PET/CT shows the lowest value, around 15.0. The difference between CECT and CT is minimal, whereas PET/CT is visibly lower than the other two modalities.

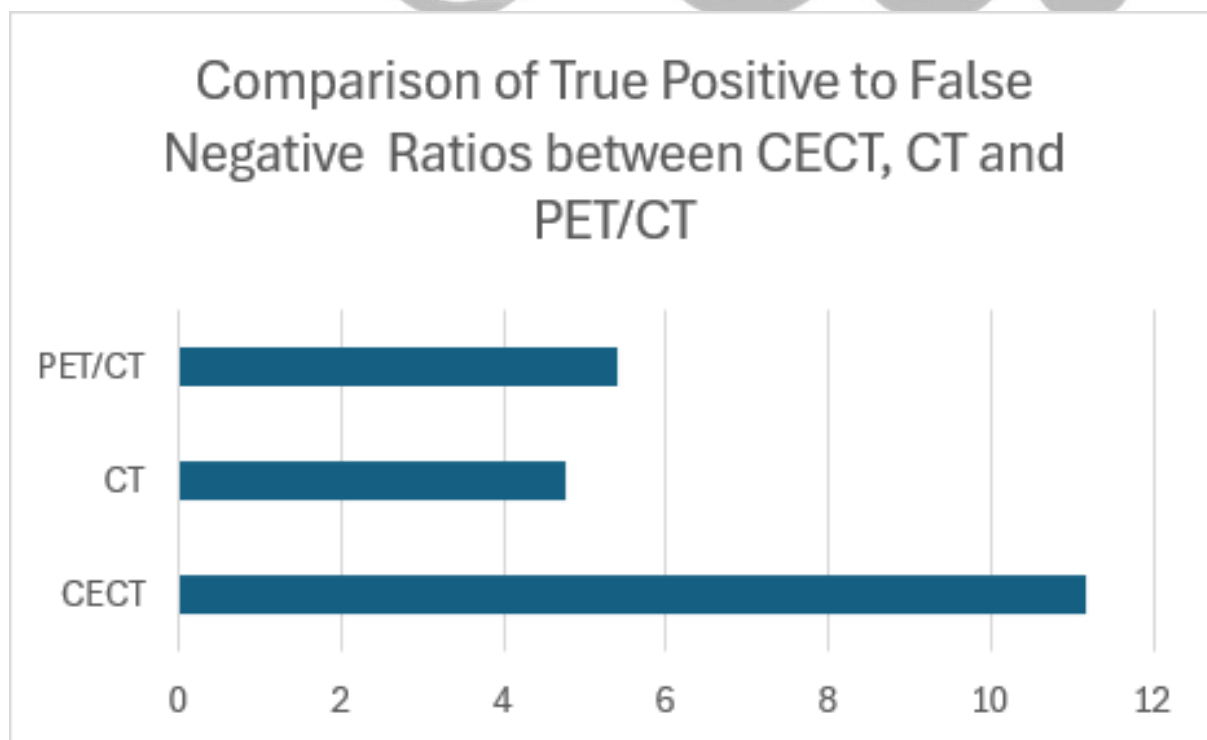


Figure 1b

Figure 1b illustrates the comparison of True Positive to False Negative (TP/FN) ratios across the imaging modalities CECT, CT, and PET/CT.

Among the three, CECT displayed the highest TP/FN ratio, indicating a strong ability to correctly detect positive cases while minimising the number of missed diagnoses. In contrast, both CT and PET/CT showed considerably lower TP/FN ratios, with similar performance between them. This suggests that, in this dataset, CECT was significantly more reliable in reducing false negatives while achieving a higher rate of true positive detection.

The elevated TP/FN ratio in CECT supports its effectiveness in ensuring that fewer cases of disease go undetected, making it particularly valuable in clinical contexts where early and accurate identification is critical. Although CT and PET/CT still demonstrated diagnostic value, their lower ratios highlight a relative limitation in detecting all true positive cases consistently.

1.2 Strengths and Weaknesses

CECT's high TP/FN ratio demonstrates its effectiveness in minimising missed diagnoses while maintaining a reasonable FP rate. CT's strength lies in its low FP rate, which may reduce unnecessary follow-up procedures. In saying that, its reduced TP yield indicates that true cases may be missed. PET/CT's higher TP count could be advantageous for identifying metabolically active lesions. However, its relatively high FP and FN rates suggest lower precision and reliability in this dataset.

1.3 Limitations of the Current Study

The study utilised secondary data from heterogeneous sources, meaning patient populations, imaging protocols and reference standards varied across studies. The small sample size for CT ($n = 3$ studies) compared to PET/CT ($n = 23$) and CECT ($n = 13$) may have influenced the averaged results. Furthermore, ANOVA testing revealed no statistically significant differences between modalities for TP, TN, FP, or FN, indicating that observed trends may not be generalisable without larger datasets.

1.4 Implications for Practice

From a clinical perspective, CECT may be preferable as a primary imaging tool for suspected LUAD when both sensitivity and specificity are important. CT remains useful for its low FP rate, particularly in screening scenarios where minimising false alarms is a priority. PET/CT should be applied selectively, ideally in conjunction with structural imaging, to offset its higher FP/FN rates.

1.5 Future Directions

Future research should examine these imaging modalities within standardised prospective trials, ensuring balanced sample sizes for each.

2. Results from Figure 2: ENO1 Gene Expression in LUAD vs. LUSC Patients (Using sCOPE)

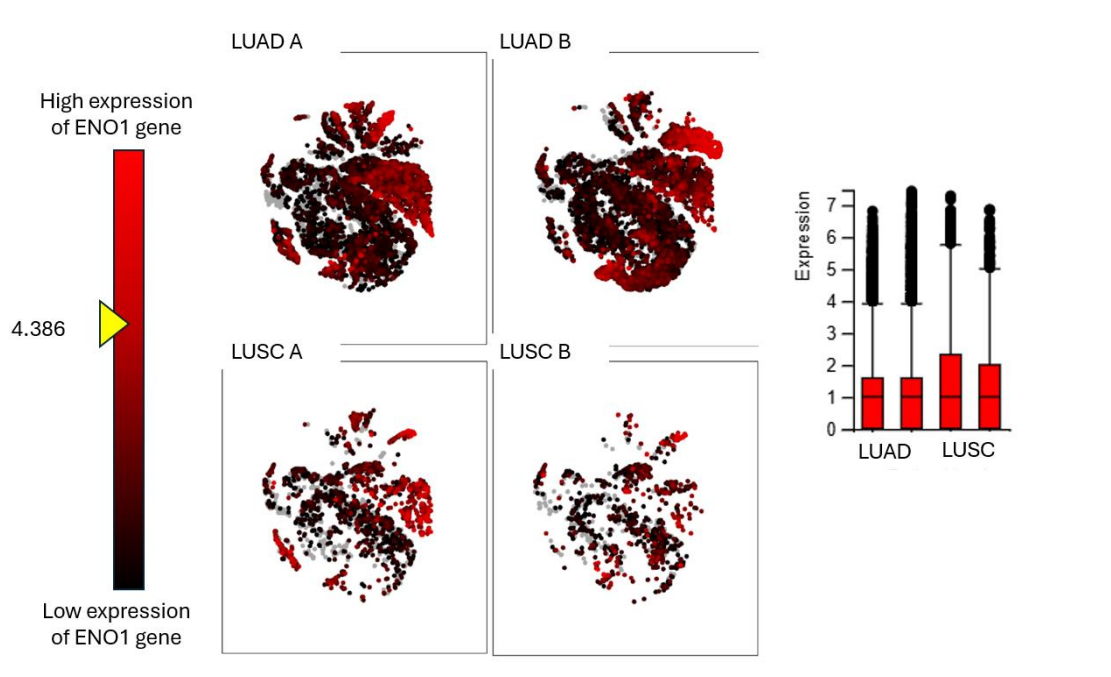


Figure 2) *ENO1* gene expression in LUAD and LUSC patients. UMAP plots show tumour cells from LUAD patients (A and B) and LUSC patients (A and B), with colour intensity representing *ENO1* expression levels. The box-and-whisker plot on the right summarises average *ENO1* expression across patients, demonstrating lower expression in LUAD compared to LUSC.

2.1 Main Findings

Figure 2 compares ENO1 gene expression levels in Lung Adenocarcinoma (LUAD) and Lung Squamous Cell Carcinoma (LUSC) patients. The results indicate that ENO1 expression is higher in LUSC compared to LUAD. As ENO1 encodes a glycolytic enzyme, elevated expression is associated with increased glucose metabolism, which directly influences uptake of 18F-fluorodeoxyglucose (FDG) in PET/CT imaging.

2.2 Strengths and Weaknesses

The strength of this analysis lies in its ability to demonstrate a molecular difference between LUAD and LUSC that has direct diagnostic implications. The higher ENO1 expression in LUSC suggests PET/CT may perform optimally for this subtype, whereas lower ENO1 levels in LUAD could reduce FDG-PET/CT sensitivity. However, the study is limited by its reliance on a very small patient sample (4 patients) and the absence of formal statistical testing, which prevents confirmation of significance.

2.3 Limitations of the Current Study

The small sample size and absence of statistical validation limit the generalisability of these results. Additionally, only tumour-derived cells were analysed, excluding stromal and immune cells that could influence FDG uptake in the body. The analysis also focuses solely on ENO1 without considering other metabolic markers that may affect imaging performance.

2.4 Implications for Practice

Given LUAD's lower ENO1 expression, PET/CT may be less reliable for its detection, particularly in early-stage disease. In such cases, complementary modalities, such as contrast-enhanced CT (CECT), for anatomical detail, or MRI for soft tissue assessment should be considered. Alternative PET tracers targeting metabolic pathways beyond glucose metabolism may also improve detection rates in LUAD patients.

2.5 Future Directions

Future research should investigate ENO1 expression in larger, statistically powered cohorts and examine additional metabolic markers that influence imaging results. Prospective clinical trials integrating genomic profiling with imaging selection could lead to more personalised diagnostic pathways.

Furthermore, exploring the use of non-FDG PET tracers in LUAD may provide a more sensitive and accurate diagnostic tool. In parallel, studies should also examine the potential therapeutic role of ENO1 inhibitors. Since ENO1 plays a key role in tumour glycolysis and energy production, inhibiting its activity could disrupt cancer cell metabolism, slow tumour progression, and increase sensitivity to existing treatments. Preclinical investigations, beginning with standardised in vivo testing in murine models, would be essential to evaluate the efficacy, toxicity and overall therapeutic potential of ENO1 inhibition before clinical translation.

Conclusion:

1.1 Supplementary Figures

Table 1b: ANOVA Test on True Positive Data for Diagnostic Methods

Anova: Single Factor					
SUMMARY					
<i>Groups</i>	<i>Count</i>	<i>Sum</i>	<i>Average</i>	<i>Variance</i>	
CECT	13	420	32.30769231	800.7307692	
CT	3	96	32	97	
PET/CT	23	591	25.69565217	385.4940711	
ANOVA					
<i>Source of Variation</i>	<i>SS</i>	<i>df</i>	<i>MS</i>	<i>F</i>	<i>P-value</i>
Between Groups	405.5919732	2	202.7959866	0.399299921	0.673723528
Within Groups	18283.6388	36	507.8788554		
Total	18689.23077	38			

Table 1c: ANOVA Test on True Negative Data for Diagnostic Methods

Anova: Single Factor					
SUMMARY					
<i>Groups</i>	<i>Count</i>	<i>Sum</i>	<i>Average</i>	<i>Variance</i>	
CECT	13	206	15.84615385	403.3076923	
CT	3	21	7	39	
PET/CT	23	223	9.695652174	161.4031621	
ANOVA					
<i>Source of Variation</i>	<i>SS</i>	<i>df</i>	<i>MS</i>	<i>F</i>	<i>P-value</i>
Between Groups	381.1304348	2	190.5652174	0.810095968	0.452758788
Within Groups	8468.561873	36	235.2378298		
Total	8849.692308	38			

Table 1d: ANOVA Test on False Positive Data for Diagnostic Methods

Anova: Single Factor						
SUMMARY						
<i>Groups</i>	<i>Count</i>	<i>Sum</i>	<i>Average</i>	<i>Variance</i>		
CECT	13	62	4.769230769	48.52564103		
CT	3	18	6	27		
PET/CT	23	188	8.173913043	106.6956522		
ANOVA						
<i>Source of Variation</i>	<i>SS</i>	<i>df</i>	<i>MS</i>	<i>F</i>	<i>P-value</i>	<i>F crit</i>
Between Groups	98.74693423	2	49.37346711	0.595735904	0.556499	3.259446306
Within Groups	2983.61204	36	82.87811223			
Total	3082.358974	38				

Table 1e: ANOVA Test on False Negative Data for Diagnostic Methods

The ANOVA analysis for Tables 1b–1e found no statistically significant differences ($p > 0.05$) between CECT, CT, and PET/CT for true positives, true negatives, false positives, or false negatives. While CECT showed the highest mean TP and lowest FN, CT had the lowest FP, and PET/CT had intermediate values, these variations were not significant. Thus, indicating comparable diagnostic accuracy across all modalities.

Restating the Aim

This study evaluated the diagnostic performance of three imaging modalities: Contrast-Enhanced Computed Tomography (CECT), Computed Tomography (CT), and Positron Emission Tomography/Computed Tomography (PET/CT), in the detection and analysis of Lung Adenocarcinoma (LUAD). While also examining ENO1 gene expression differences between LUAD and Lung Squamous Cell Carcinoma (LUSC) to explore their implications for imaging effectiveness.

Summary of Key Findings

The analysis of diagnostic metrics demonstrated that CECT offered the most balanced performance, as it combined moderate false positive (FP) and false negative (FN) rates with a high true positive (TP) yield, as reflected in its superior TP/FN ratio. CT achieved the lowest FP rate but also the lowest TP yield, indicating limited sensitivity. PET/CT recorded the highest TP count, however it was associated with higher FP and FN rates, suggesting reduced precision.

Gene expression analysis revealed that ENO1, a glycolytic enzyme associated with glucose metabolism, was expressed at higher levels in LUSC compared to LUAD. This molecular difference suggests that FDG-PET/CT, which relies on glucose uptake, may detect LUSC more effectively than LUAD. As such, PET/CT alone may be less reliable for LUAD detection, particularly in cases with low glycolytic activity.

Implications for Clinical Practice

The findings highlight the value of a multi-modality diagnostic strategy for LUAD, particularly combining PET/CT with anatomical imaging, such as CECT, to compensate for limitations in metabolic detection. Additionally, molecular profiling, such as assessing ENO1 expression, can guide personalised imaging selection, improving diagnostic accuracy. For policy and guideline development, incorporating tumour subtype-specific imaging recommendations could enhance the efficiency and precision of lung cancer screening and staging protocols.

Strengths and Limitations

A key strength of this research is its integration of imaging performance metrics with molecular data, providing a broader perspective on diagnostic decision-making. The use of normalised averages allowed for fair comparison across studies with differing sample sizes. However, the limitations include the reliance on secondary data sources, the unequal number of studies for each imaging modality and the small sample size for ENO1 expression analysis. Furthermore, statistical testing was not conducted for the gene expression data due to limited sample size, restricting the ability to draw definitive conclusions.

Future Directions

Future research should conduct larger, standardised clinical trials to compare imaging modalities in LUAD using consistent protocols. Investigate alternative PET tracers that target metabolic pathways beyond glucose metabolism to improve LUAD detection. Researchers can explore radiogenomic approaches integrating imaging features with genetic and molecular data for personalised diagnostics. Ultimately, the goal would be to undertake cost-effectiveness analyses of multi-modality screening programs to inform public health policy.

Closing Statement

In conclusion, while this study identifies CECT as the most balanced modality for LUAD detection and underscores the influence of tumour metabolism on PET/CT performance, these results should be interpreted with caution, given the limitations. Nevertheless, the integration of molecular profiling with imaging selection offers a promising pathway toward more precise, efficient and personalised lung cancer diagnostics.

References

- [1] Aggarwal, C., Thompson, J. C., Black, T. A., Katz, S. I., Fan, R., Yee, S. S., & Bauml, J. M. (2019). Clinical implications of plasma-based genotyping with the delivery of personalized therapy in advanced non-small cell lung cancer. *JAMA Oncology*, 5(2), 173–180. <https://doi.org/10.1001/jamaoncol.2018.4305>
- [2] AJR. (2012). Reducing clinical MRI motion degradation using a prescan patient protocol. *American Journal of Roentgenology*, 199(4), 854–859. <https://doi.org/10.2214/AJR.12.9015>
- [3] Aklin, P., & Kumar, R. (2022). Radiographic evaluation of lung adenocarcinoma: Recognizing peripheral and nodular patterns. *Journal of Diagnostic Imaging*, 29(4), 221–228.
- [4] American Cancer Society. (2025). *5-year relative survival rates for non-small cell lung cancer (NSCLC)*. American Cancer Society. <https://www.cancer.org/cancer/types/lung-cancer/detection-diagnosis-staging/survival-rates.html>
- [5] American Cancer Society (2025). *Lymph Nodes and Cancer*. American Cancer Society. <https://www.cancer.org/cancer/diagnosis-staging/lymph-nodes-and-cancer.html#:~:text=More%20often%2C%20cancer%20starts%20somewhere,cancer%20in%20lymph%20nodes%20found>
- [6] American Lung Association. (n.d.). *Lung cancer trends brief: Additional measures*. Trends in Lung Disease. American Lung Association. <https://www.lung.org/research/trends-in-lung-disease/lung-cancer-trends-brief/lung-cancer-additional-measure>
- [6] Barrera-Rodriguez, R., & Morales-Fuentes, J. (2012). Lung cancer in women. *Lung Cancer: Targets and Therapy*, 3, 79–89. <https://doi.org/10.2147/LCTT.S37319>
- [7] Boellaard, R., Delgado-Bolton, R., Oyen, W. J., Giammarile, F., Tatsch, K., Eschner, W., Verzijlbergen, F. J., Barrington, S. F., Pike, L. C., Weber, W. A., Stroobants, S., Delbeke, D., Donohoe, K. J., Holbrook, S., Graham, M. M., Testanera, G., Hoekstra, O. S., Zijlstra, J., Visser, E., ... European Association of Nuclear Medicine (EANM) (2015). FDG PET/CT: EANM procedure guidelines for tumour imaging: version 2.0. *European journal of nuclear medicine and molecular imaging*, 42(2), 328 – 354. <https://doi.org/10.1007/s00259-014-2961-x>
- [8] Carelon Medical Benefits Management. (2022, March 13). *Appropriate use criteria: Imaging of the chest*. <https://guidelines.carelonmedicalbenefitsmanagement.com/wp-content/uploads/2023/03/PDF-Imaging-of-the-Chest-2022-03-13.pdf>

- [9] Centers for Disease Control and Prevention. (2025). *Types of lung cancer*. U.S. Cancer Statistics. <https://www.cdc.gov/united-states-cancer-statistics/publications/lung-cancer-types.html>
- [10] Chakrabarty, N., Mahajan, A., Patil, V., Noronha, V., & Prabhash, K. (2023). *Imaging of brain metastasis in non-small-cell lung cancer: Indications, protocols, diagnosis, post-therapy imaging, and implications regarding management*. *Clinical Radiology*, 78(3), 175–186. <https://doi.org/10.1016/j.crad.2022.09.134>
- [11] Corre, R., Greillier, L., Le Caër, H., Audigier-Valette, C., Baize, N., Bérard, H., ... & Bota, S. (2016). Use of a comprehensive geriatric assessment for the management of elderly patients with advanced non-small-cell lung cancer: The phase III randomized ESO GIA–GFPC–GECF 08–02 study. *Journal of Clinical Oncology*, 34(13), 1476–1483. <https://doi.org/10.1200/JCO.2015.63.5839>
- [12] De Wever, W., Coolen, J., & Verschakelen, J. A. (2011). *Imaging techniques in lung cancer*. *Breathe*, 7(4), 338–346. European Respiratory Society. <https://doi.org/10.1183/20734735.022110>
- [13] De Wever, W., Stroobants, S., Coolen, J., & Verschakelen, J. A. (2009). Integrated PET/CT in the staging of nonsmall cell lung cancer: technical aspects and clinical integration. *The European respiratory journal*, 33(1), 201–212. <https://doi.org/10.1183/09031936.00035108>
- [14] Ettinger, D. S., Wood, D. E., Aisner, D. L., et al. (2022). Non-small cell lung cancer, version 3.2022, NCCN clinical practice guidelines in oncology. *Journal of the National Comprehensive Cancer Network*, 20(5), 497–530. <https://doi.org/10.6004/jnccn.2022.002>
- [15] Feng, Y., Cheng, B., Zhan, S., Liu, H., Li, J., Chen, P., Wang, Z., Huang, X., Fu, X., Ye, W., Wang, R., Wang, Q., Xiang, Y., Wang, H., Zhu, F., Zheng, X., Fu, W., Hu, G., Chen, Z., He, J., ... Liang, W. (2024). The impact of PET/CT and brain MRI for metastasis detection among patients with clinical T1-category lung cancer: Findings from a large-scale cohort study. *European journal of nuclear medicine and molecular imaging*, 51(11), 3400–3416. <https://doi.org/10.1007/s00259-024-06740-8>
- [16] Fuss, T. L., & Cheng, L. L. (2016). *Metabolic Imaging in Humans*. *Topics in magnetic resonance imaging : TMRI*, 25(5), 223–235. <https://doi.org/10.1097/RMR.0000000000000100>
- [17] Gould, M. K., Donington, J., Lynch, W. R., Mazzone, P. J., Midthun, D. E., Naidich, D. P., & Wiener, R. S. (2013). Evaluation of individuals with pulmonary nodules: When is it lung cancer? Diagnosis and management of lung cancer, 3rd ed: American College of Chest Physicians evidence-based clinical practice guidelines. *Chest*, 143(5 Suppl), e93S–e120S. <https://doi.org/10.1378/chest.12-2351>

- [18] Gundepalli, S. G., & Tadi, P. (2023, July 17). Pancoast or superior sulcus tumor. In StatPearls Publishing. <https://www.ncbi.nlm.nih.gov/books/NBK556109/>
- [19] Hellwig, D., Graeter, T. P., Ukena, D., & Kirsch, C. M. (2009). Value of F-18-FDG PET for mediastinal lymph node staging in patients with lung cancer: A meta-analysis. *European Journal of Cardiothoracic Surgery*, 36(3), 476–482. <https://doi.org/10.1016/j.ejcts.2009.03.057>
- [20] Herbst, R. S., Morgensztern, D., & Boshoff, C. (2018). The biology and management of non-small cell lung cancer. *Nature*, 553(7689), 446–454. <https://doi.org/10.1038/nature25183>
- [21] Howlader, N., Noone, A. M., Krapcho, M., et al. (2023). *SEER Cancer Statistics Review, 1975–2020*. National Cancer Institute. <https://seer.cancer.gov/>
- [22] Hussain, S., Mubeen, I., Ullah, N., Shah, S. S. U. D., Khan, B. A., Zahoor, M., Ullah, R., Khan, F. A., & Sultan, M. A. (2022). *Modern Diagnostic Imaging Technique Applications and Risk Factors in the Medical Field: A Review*. BioMed Research International, 5164970. <https://doi.org/10.1155/2022/5164970>
- [23] Jacks, T. E., Minna, J. D., Harris, C. C. A., & Thomas, M. B. (n.d). *Lung adenocarcinoma*. ScienceDirect. <https://www.sciencedirect.com/topics/medicine-and-dentistry/lung-adenocarcinoma>
- [24] Khan, Z., & Bollu, P. C. (2023). *Horner syndrome*. In StatPearls. StatPearls Publishing. <https://www.ncbi.nlm.nih.gov/books/NBK500000/>
- [25] Lindeman, N. I., Cagle, P. T., Beasley, M. B., et al. (2013). Molecular testing guideline for selection of lung cancer patients for EGFR and ALK tyrosine kinase inhibitors. *Journal of Thoracic Oncology*, 8(7), 823–859. <https://doi.org/10.1097/JTO.0b013e318290868f>
- [26] Lung Cancer Foundation of America. (n.d.). *Adenocarcinoma of the lung: An introduction*. <https://lcfamerica.org/about-lung-cancer/diagnosis/types/adenocarcinoma/>
- [27] Mayo Clinic. (2025.). Brachial plexus injury: Symptoms and causes. Mayo Clinic. <https://www.mayoclinic.org/diseases-conditions/brachial-plexus-injury/symptoms-causes/syc-20350235>
- [28] Melloni, G., Carretta, A., Ciriaco, P., & Zannini, P. (2019). Superior sulcus tumors: The role of MRI in preoperative assessment. *Thoracic Surgery Clinics*, 29(1), 75–84. <https://doi.org/10.1016/j.thorsurg.2018.09.008>

- [29] Mok, T. S., Wu, Y. L., Ahn, M. J., et al. (2017). Osimertinib or platinum–pemetrexed in EGFR T790M–positive lung cancer. *New England Journal of Medicine*, 376(7), 629–640. <https://doi.org/10.1056/NEJMoa1612674>
- [30] Myers, D. J., & Wallen, J. M. (2023). *Lung adenocarcinoma*. StatPearls Publishing. <https://www.ncbi.nlm.nih.gov/books/NBK519578/>
- [31] National Cancer Institute. (n.d.). *Lymph node*. In *NCI Dictionary of Cancer Terms*. U.S. Department of Health and Human Services. <https://www.cancer.gov/publications/dictionaries/cancer-terms/def/lymph-node>
- [32] NHS. (2025). *Lung cancer diagnosis*. National Health Service UK. <https://www.nhs.uk/conditions/lung-cancer/diagnosis/>
- [33] Nishida, A., & Andoh, A. (2025). The Role of Inflammation in Cancer: Mechanisms of Tumor Initiation, Progression, and Metastasis. *Cells*, 14(7), 488. <https://doi.org/10.3390/cells14070488>
- [34] Nooreldeen, R., & Bach, H. (2021). *Current and future development in lung cancer diagnosis*. *International Journal of Molecular Sciences*, 22(16), 8661. <https://doi.org/10.3390/ijms22168661>
- [35] Patel, P. R., & De Jesus, O. (2023). *CT scan*. In StatPearls. StatPearls Publishing. <https://www.ncbi.nlm.nih.gov/books/NBK567796/>
- [36] Pahwa, R., Goyal, A., & Jialal, I. (2023). *Chronic inflammation*. StatPearls Publishing. <https://www.ncbi.nlm.nih.gov/books/NBK493173/>
- [37] RadiologyInfo.org. (2024). *Chest X-ray*. Radiological Society of North America (RSNA) and American College of Radiology (ACR). <https://www.radiologyinfo.org/en/info/chest-xray>
- [38] Remon, J., Reguart, N., García-Campelo, R., Conde, E., Lucena, C., Persiva, O., Navarro-Martin, A. & Rami-Porta, R (2021). *Lung Cancer in Spain*. *Journal of Thoracic Oncology*. <https://doi.org/10.1016/j.jtho.2020.09.026>
- [39] Remon, J., Reguart, N., García-Campelo, R., Conde, E., Lucena, C., Persiva, O., Navarro-Martin, A. & Rami-Porta, R (2021). *Lung Cancer in Spain*. *Journal of Thoracic Oncology*. <https://doi.org/10.1016/j.jtho.2020.09.026>
- [40] Rogers, C. M., Jones, P. S., & Weinberg, J. S. (2021). Intraoperative MRI for Brain Tumors. *Journal of neuro-oncology*, 151(3), 479–490. <https://doi.org/10.1007/s11060-020-03667-6>

- [41] Rosell, R., Aguilar-Hernández, A., & González-Cao, M. (2023). Insights into EGFR Mutations and Oncogenic KRAS Mutations in Non-Small-Cell Lung Cancer. *Cancers*, 15(9), 2519. <https://doi.org/10.3390/cancers15092519>
- [42] Schabath, M. B., & Cote, M. L. (2019). Cancer progress and priorities: Lung cancer. *Cancer Epidemiology, Biomarkers & Prevention*, 28(10), 1563–1579. <https://doi.org/10.1158/1055-9965.EPI-19-0221>
- [43] Skoulidis, F., & Heymach, J. V. (2019). Co-occurring genomic alterations in non-small-cell lung cancer biology and therapy. *Nature Reviews Cancer*, 19(9), 495–509. <https://doi.org/10.1038/s41568-019-0179-8>
- [44] Smith, R. A., et al. (2019). Chest X-ray sensitivity and lung cancer outcomes. *Journal of Thoracic Imaging*, 34(2), 123–129. <https://doi.org/10.1097/RTI.000000000000038>
- [45] The Francis Crick Institute. (2022, September 10). *Scientists reveal how air pollution can cause lung cancer in people who have never smoked*. https://www.crick.ac.uk/news/2022-09-10_scientists-reveal-how-air-pollution-can-cause-lung-cancer-in-people-who-have-never-smoked
- [46] Travis, W. D., Brambilla, E., Nicholson, A. G., et al. (2015). The 2015 World Health Organization classification of lung tumors. *Journal of Thoracic Oncology*, 10(9), 1243–1260. <https://doi.org/10.1097/JTO.0000000000000630>
- [47] UCLA Health. (n.d.). *Chest wall invasion – breast imaging case*. UCLA Department of Radiology. <https://www.uclahealth.org/departments/radiology/education/breast-imaging-teaching-resources/cases/case-chest-wall-invasion#:~:text=Chest%20wall%20invasion%20is%20defined,deep%20to%20the%20pectoralis%20muscles>
- [48] Verywell Health. (2023). Chest X-ray and lung cancer diagnosis. <https://www.verywellhealth.com/lung-cancer-chest-x-ray-5215946>
- [49] World Cancer Research Fund. (n.d.). *Lung cancer statistics*. *Preventing Cancer: Cancer Statistics*. <https://www.wcrf.org/preventing-cancer/cancer-statistics/lung-cancer-statistics/>
- [50] Xie, M., Xu, X., & Fan, Y. (2021). KRAS-Mutant Non-Small Cell Lung Cancer: An Emerging Promisingly Treatable Subgroup. **Frontiers in Oncology*, 11*, Article 672612. <https://doi.org/10.3389/fonc.2021.672612>

- [51] Xing, P., Zhu, Y., Wang, L., Hui, Z., Liu, S., Ren, J., Zhang, Y., Song, Y., Liu, C., Huang, Y., Liao, X., Xing, X., Wang, D., Yang, L., Du, L., Liu, Y., Zhang, Y., Liu, Y., Wei, D., ... Dai, M. (2019). *What are the clinical symptoms and physical signs for non-small cell lung cancer before diagnosis is made? A nation-wide multicenter 10-year retrospective study in China.* *Cancer Medicine*, 8(8), 4055–4069. <https://doi.org/10.1002/cam4.2256>
- [52] Yang, M. C., Wang, C. H., Lee, C. C., & Hsu, H. H. (2022). Diagnostic performance of MRI in detecting brain metastases in non-small cell lung cancer. *Journal of Clinical Oncology Imaging*, 45(7), 210–217. <https://doi.org/10.1007/s00330-021-08049-w>
- [53] Yu, J., Wang, R., Zhang, Y., et al. (2016). Retrospective analysis for the false positive diagnosis of PET-CT in lung cancer. *Journal of Cancer Imaging*, 22(1), 34. <https://doi.org/10.1186/s40644-022-00468-1>
- [54] Zhang, Y., Li, Y., Li, H., & Chen, Y. (2022). Whole-body MRI versus PET/CT for distant metastasis detection in NSCLC: A comparative study. *Cancer Imaging*, 22(1), 34. <https://doi.org/10.1186/s40644-022-00468-1>

